Digital Communications and Networks (2015) 1, 141–151

HOSTED BY

ELSEVIER

Available online at www.sciencedirect.com

ScienceDirect

journal homepage: www.elsevier.com/locate/dcan

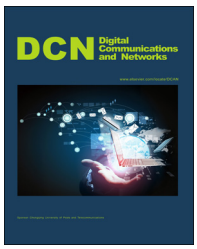

A novel approach to gait synchronization and transition for reconfigurable walking platforms



Shunsuke Nansai[a], Nicolas Rojas[b], Mohan Rajesh Elara[c,*], Ricardo Sosa[c], Masami Iwase[d]

[a]*Department of Advanced Multidisciplinary Engineering, Tokyo Denki University, Japan*
[b]*Department of Mechanical Engineering and Materials Science, Yale University, USA*
[c]*Engineering Product Development Pillar, Singapore University of Technology and Design, Singapore*
[d]*Department of Robotics and Mechatronics, Tokyo Denki University, Japan*

Received 9 February 2015; received in revised form 15 April 2015; accepted 18 April 2015
Available online 11 May 2015

KEYWORDS
Legged robot;
Static stability;
Reconfigurable mechanism;
Jansen mechanism;
Walking platform

Abstract
Legged robots based on one degree-of-freedom reconfigurable planar leg mechanisms, that are capable of generating multiple useful gaits, are highly desired due to the possibility of handling environments and tasks of high complexity while maintaining simple control schemes. An essential consideration in these reconfigurable legged robots is to attain stability in motion, at rest as well as while transforming from one configuration to another with the minimum number of legs as long as the full range of their walking patterns, resulting from the different gait cycles of their legs, is achieved. To this end, in this paper, we present a method for the generation of input joint trajectories to properly synchronize the movement of quadruped robots with reconfigurable legs. The approach is exemplified in a four-legged robot with reconfigurable Jansen legs capable of generating up to six useful different gait cycles. The proposed technique is validated through simulated results that show the platform's stability across its six feasible walking patterns and during gait transition phases, thus considerably extending the capabilities of the non-reconfigurable design.
© 2015 Chongqing University of Posts and Telecommunications. Production and Hosting by Elsevier B.V.
This is an open access article under the CC BY-NC-ND license (http://creativecommons.org/licenses/by-nc-nd/4.0/).

1. Introduction

Legged robots have always been a preferred choice for a variety of applications like search and rescue given their versatile and rugged locomotion capabilities. The choice of legged mechanisms often responds to design requirements such as the ability to move through irregular terrains or to increase stability, maneuverability or energy efficiency.

*Corresponding author.
E-mail addresses: nansai@ctrl.fr.dendai.ac.jp (S. Nansai), nicolas.rojas@yale.edu (N. Rojas), rajeshelara@sutd.edu.sg (M.R. Elara), ricardo_sosa@sutd.edu.sg (R. Sosa), iwase@fr.dendai.ac.jp (M. Iwase).

http://dx.doi.org/10.1016/j.dcan.2015.04.003
2352-8648/© 2015 Chongqing University of Posts and Telecommunications. Production and Hosting by Elsevier B.V. This is an open access article under the CC BY-NC-ND license (http://creativecommons.org/licenses/by-nc-nd/4.0/).

However, any valid gait reconfiguration – *i.e.*, a useful change of walking pattern – in these legged robots poses numerous opportunities as well as research challenges. Legged animals coordinate a wide range of components and systems to walk adaptively and efficiently under a variety of speeds, terrains and task goals including chasing, courtship and stealth.

The robotics literature shows a variety of design strategies to generate different gait patterns in legged robots, including, to name a few: structural combination of rigid and tensile structural elements [1], morphological computation [2], oscillator controller with pneumatic actuators [3] and biomimetic adaptations based on ground contact timing [4] or using sensorimotor coordination [5]. Alternatively, walking platforms based on one degree-of-freedom reconfigurable planar leg mechanisms, that are capable of generating multiple useful gaits, while maintaining simple control schemes can also be proposed. For example, in [6], a reconfigurable Jansen leg that varies its hardware morphology to produce a wide set of novel gaits by parametric changes of its components and subassemblies was discussed. To ensure safe locomotion across a difficult terrain, a robot must be able to stably switch between gaits either at rest or in motion. Literature points a number of efforts to this end, [7] proposes an approach based on acyclic feed forward motion patterns that allow a robot to switch from one gait to another. Ref. [8] applies nonlinear oscillators to model Central Pattern Generators (CPGs) that is able to initiate/stop locomotion; generate different gaits, and to easily select and switch between the different gaits according to the speed and/or the behavioral context. Ref. [9] attempts to induce a quadruped robot to walk and switch gaits dynamically on irregular terrain and run on flat terrain by using a nervous system model.

A fundamental problem of the gait reconfiguration solutions based on reconfigurable legged robots is to reach stability both in motion and rest, as well as while transforming from one configuration to another with the minimum number of legs, while the complete range of walking patterns is available. In this paper, we discuss a method for the proper generation of input joint trajectories to synchronize the different gait cycles and gait transitions of quadruped robots with one degree-of-freedom reconfigurable legs. In order to exemplify our approach, we focus on a four-legged robot with reconfigurable Jansen legs (Fig. 1). Theoretically, such walking platform is capable of generating up to six useful different walking patterns, resulting from the different gait cycles of a reconfigurable Jansen leg. It will be shown how, by using the proposed technique, all these feasible patterns can be successfully attained. In this way, the capabilities of a quadruped robot based on standard non-reconfigurable Jansen legs are considerably extended. In particular, the synchronization and the gait transitions are realized by utilizing a trajectory generator based on fifth-polynomial interpolation. Our presented reconfigurable platform, a novel approach of reconfigurable robot contained within a nested reconfigurable concept [10], needs applications for the synchronization for walking as well as the gait transitions between the gait patterns. However, to design applications for each synchronization and each gait transition is meaningless due to infinite complexities. Hence, the biggest challenge of this paper is to achieve these with the simplest application as much as possible. This paper reports that all synchronization and gait transitions can be achieved by only one gait generator by utilizing fifth-polynomial interpolation.

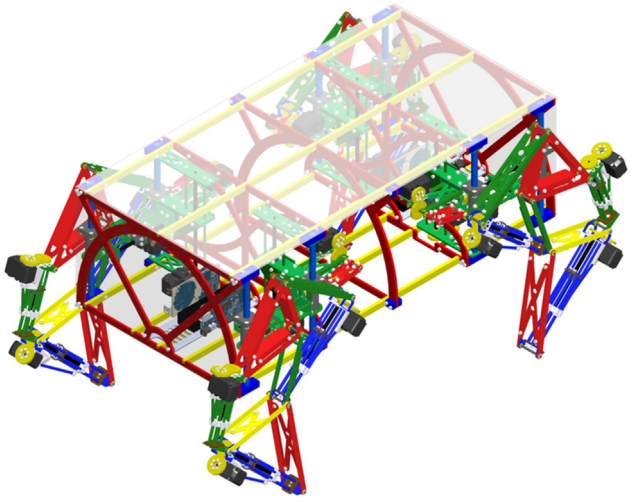

Fig. 1 Legged robots based on one degree-of-freedom reconfigurable planar leg mechanisms may operate in environments and tasks of high complexity while maintaining simple control schemes. This four-legged robot is based on reconfigurable Jansen legs capable of generating up to six different gait cycles.

The rest of the paper is organized as follows. Section 2 presents the specifications of the reconfigurable Jansen platform under test. Section 3 deals with the formulation of the trajectory generator. Section 4 puts forward the synchronization strategy for coordinating multiple leg movements to achieve the six distinct stable walking patterns. Section 5 presents the static stability analysis of the synthesized walking gaits. Detailed characterization of the realized gait transitions for both static and dynamic cases are dealt in Section 6. Static stability analysis of the gait transitions is presented in Section 7. Finally, section 8 concludes this study.

2. Specification of the reconfigurable Jansen platform

In this section, specifications of a developed reconfigurable Jansen legged robot are discussed. This reconfigurable walking platform is used herein as case study for the generation of input joint trajectories to synchronize multiple reconfigurable one-degree-of-freedom legs for realizing stable walking gaits.

In a previous study, we reported a reconfigurable approach to robotic legged locomotion that produces a wide variety of gait curves, opening new possibilities for innovative applications [6]. Such robot can vary its hardware morphology by parametric changes of its link lengths. In particular, this reconfigurable linkage switches from a pin-jointed Grübler kinematic chain to a five degree-of-freedom mechanism with slider joints during the reconfiguration process. The identified novel gait patterns are shown in Table 1.

An essential consideration in most legged platforms that determines the required number of legs is the ability to attain stability both in motion and rest. Previous works related to legged platforms based on standard non-reconfigurable Jansen legs have overcome the stability issues by utilizing more than four legs – *e.g.* [14]. However, increasing the number of legs gives rise to a range of other problems including greater cost and size, a more complex electro-mechanical control system,

Table 1 The identified novel gait patterns.

Default curve	Digitigrade locomotion	Obstacle avoidance
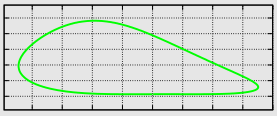	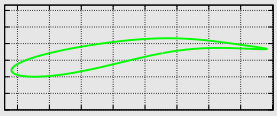	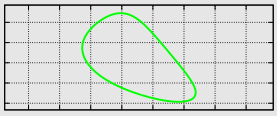
It is interesting to note that the standard foot trajectory of a Jansen leg resembles to the plantigrade locomotion of some terrestrial animals. In fact, this trajectory is quite similar to those of the ankles of rats [11].	The shape of this curve is quite similar to the gait cycle of a cat [12, Fig. 2]. Digitigrades tend to be very fast runners [13].	In this case, the height of the foot trajectory is a 36.74% of the total height of the leg
Jam avoidance	**Step climbing**	**Drilling motion**
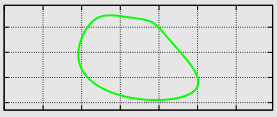	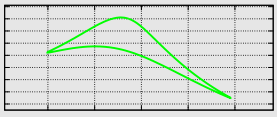	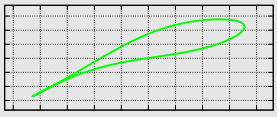
This type of trajectory is of interest because facing the soil with an arc shape, allows to look for a suitable support point at the same time	This gamma-like pattern is appropriate for climbing steps	This curve is of interest because its needle-like shape can be used for drilling activities

and maintenance issues. This problem becomes even more evident in the case of reconfigurable design approaches that realize different gaits via, for instance, changing dimensions of a set of links in the legs. Then, any increase in the number of legs directly contribute to the complexity of the entire system.

Given the discussed factors, the development of reconfigurable walking platforms with a minimum number of legs is a must. However, reconfigurable designs with less than four legs should be avoided in order to maintain simplicity and evade the related considerations of Zero Moment Point (ZMP) approaches for achieving static and/or dynamic stability [15-17]. In addition, in Jansen platforms, previous studies have shown the need to account for toe slipping while realizing walking patterns due to difference in speeds at which each leg moves [18]. Therefore, a ZMP-centered solution seems inappropriate. In consequence, a four-legged reconfigurable Jansen platform is considered for the analysis discussed in this work.

A novel mechanical approach for achieving dynamic walking stability in a standard four-legged Jansen platform has been previously proposed and validated [19]. In this approach, a special gear system is designed to enable 3 point leg contact with the ground surface at any time during the walking process, thus achieving stability. However, adopting the mechanical approach in a reconfigurable Jansen platform would require an additional gear module for each new gait produced or every configuration of the robot. An alternative control theoretic approach is here adopted to overcome the need for additional gear modules and associated mechanical complexities to achieve walking stability.

Fig. 1 shows the CAD design of a four-legged reconfigurable Jansen platform. For details of the reconfigurable Jansen leg and its different gait cycles, the interested reader is addressed to [6]. In this robot, which possesses reconfigurable capabilities that result from the six gait patterns presented in Table 1, each leg is controlled independently by a rotary actuator. In the next section, the formulation for the trajectory generation of input joints is presented.

3. Design of the trajectory generator

A fifth degree polynomial interpolation generates a smooth trajectory from a starting point of a gait to an ending point as the speed and the acceleration are represented as fourth and third degrees respectively. Since, all trajectory parameters (position, speed and acceleration) in this approach are represented as a continuous function, load forces to the actuators can be decreased. Given these advantages, we use this technique for our generation of trajectories, an approach that has been successfully used previously in the community [20-22].

The trajectories of position $r(t)$, speed $\dot{r}(t)$ and acceleration $\ddot{r}(t)$ in terms of time t are defined as follows:

$$r(t) = a_5 t^5 + a_4 t^4 + a_3 t^3 + a_2 t^2 + a_1 t + a_0, \tag{1}$$

$$\dot{r}(t) = 5a_5 t^4 + 4a_4 t^3 + 3a_3 t^2 + 2a_2 t + a_1, \tag{2}$$

$$\ddot{r}(t) = 20a_5 t^3 + 12a_4 t^2 + 6a_3 t + 2a_2, \tag{3}$$

where a_i $(i = 0, \ldots, 5)$ represents coefficients and these are derived from initial states and final states of a given gait. The initial and the final states are defined as x_s and x_f respectively, and let a transformation time T (s) be constant. Using Eqs. (1)-(3), the initial states at the starting time, a_0, a_1 and a_2, are derived as follows:

$$r(0) = a_0 = x_s, \tag{4}$$

$$\dot{r}(0) = a_1 = \dot{x}_s, \tag{5}$$

$$\ddot{r}(0) = 2a_2 = \ddot{x}_s. \tag{6}$$

Also, from the relation of the final states at the ending time, we have

$$r(T) = a_5 T^5 + a_4 T^4 + a_3 T^3 + a_2 T^2 + a_1 T + a_0 = x_f, \tag{7}$$

$$\dot{r}(T) = 5a_5 T^4 + 4a_4 T^3 + 3a_3 T^2 + 2a_2 T + a_1 = \dot{x}_f, \tag{8}$$

$$\ddot{r}(T) = 20a_5 T^3 + 12a_4 T^2 + 6a_3 T + 2a_2 = \ddot{x}_f. \tag{9}$$

By representing Eqs. (7)-(9) as a matrix form, a_3, a_4 and a_5 are derived as follows:

$$\begin{bmatrix} a_5 \\ a_4 \\ a_3 \end{bmatrix} = A^{-1} \begin{bmatrix} x_f - x_s - \dot{x}_s T - \frac{\ddot{x}_s}{2} T^2 \\ \dot{x}_f - \dot{x}_s - \ddot{x}_s T \\ \ddot{x}_f - \ddot{x}_s \end{bmatrix} \tag{10}$$

where

$$A = \begin{bmatrix} T^5 & T^4 & T^3 \\ 5T^4 & 4T^3 & 3T^2 \\ 20T^3 & 12T^2 & 6T \end{bmatrix}$$

Our strategy for synchronization and gait transition is designed based on the trajectory generator presented in this section. As the fifth degree polynomial interpolation can be calculated uniquely depending upon the initial conditions x_s, the final conditions x_f and the transformation time T, the synchronization and the gait transition strategy is therefore designed by defining these states. And, it is shown that the synchronization and the gait transitions are realized by utilizing only this gait generator designed in this section.

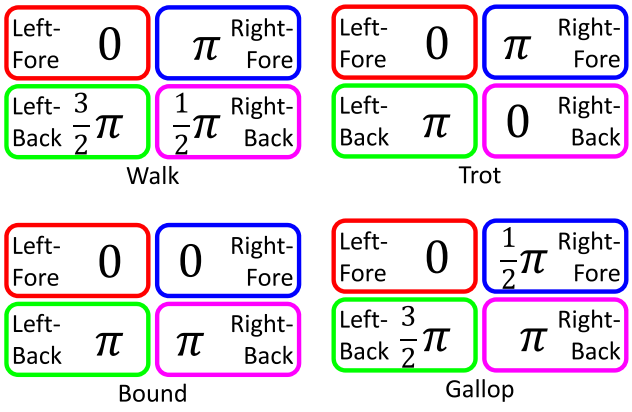

Fig. 2 Walking patterns in quadruped robots.

4. Synchronization

A leg synchronization strategy for realizing a set of stable walking gaits in reconfigurable quadruped Jansen platform is proposed. Several locomotion patterns are available from the literature for the case of a general quadruped robot as shown in Fig. 2 (adapted from [23]). Particularly, in this work, we focus on the synchronization strategy for the "walk" pattern. The other three patterns, that involve situations wherein only two legs contact the ground surface, are left for future work.

From Fig. 2, it can observed that in walk there is a switch of the idling leg with phase of 90 degrees, and the switching sequence of the idling leg is "Left-Fore" → "Right-Back" → "Right-Fore" → "Left-Back" → "Left-Fore" →, and so on. It could be concluded as well that the state sequences for the walk pattern has a constant phase, if the idling leg is assumed as a state. We use the trajectory generator introduced in Section 3 to produce trajectories to move from one state to the next one. Note that, since the walking platform under study is based on a one degree-of-freedom reconfigurable linkage, there is no need of a stabilization controller for the resulting trajectories.

Since the height of a leg in a platform that is based on a Jansen linkage depends only on the angle of the driving link, the angle of the input joint, say θ, the support leg and the idling leg can be switched depending on the value of such angle. In addition, the state transition can also be

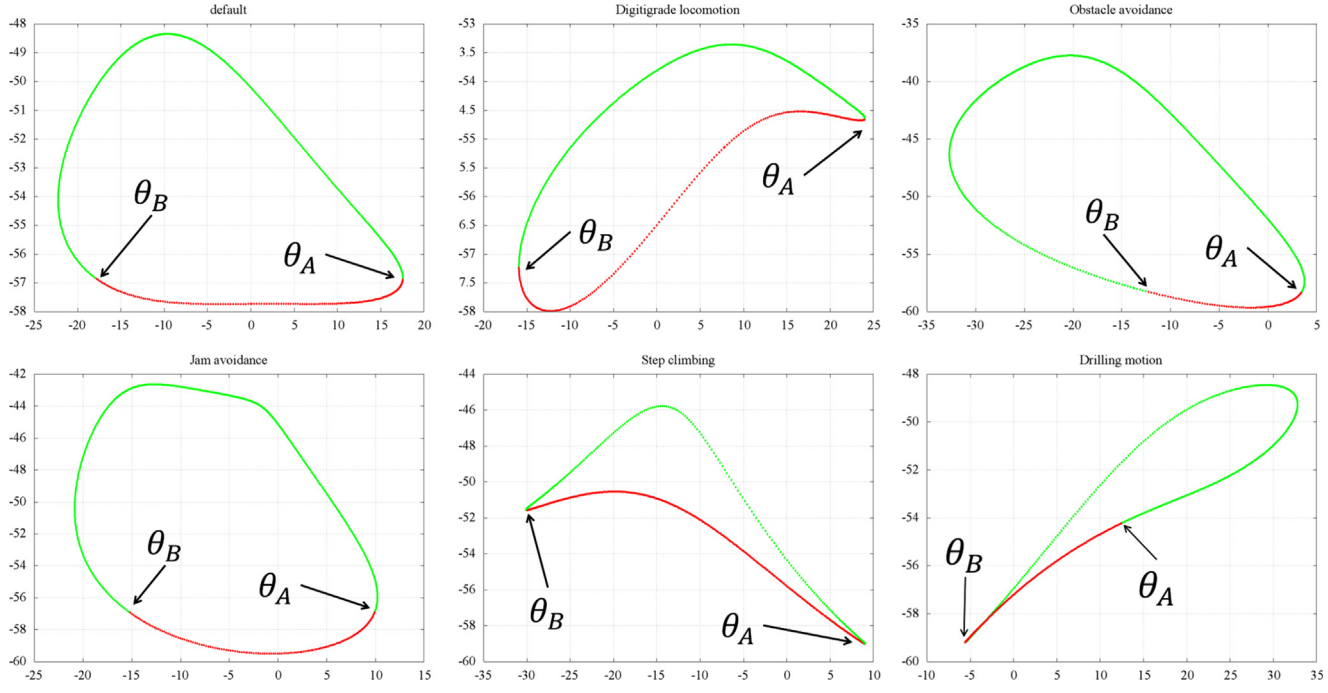

Fig. 3 The switching angles of support leg and idling leg. The red and green curves represent the sections of the support leg and idling leg, respectively.

controlled by the angle of the driving link. For the purpose of defining the order of the states through naming convention, we define the states of the idling leg "Left-Fore", "Right-Back", "Right-Fore" and "Left-Back" as "PHASE 1", "PHASE 2", "PHASE 3", and "PHASE 4", respectively. The switch angles of the support and idling legs for gaits presented in Table 1 are presented in Fig. 3 and Table 2.

In Fig. 3, θ_A and θ_B are defined by the nature of each individual gait pattern. For the "default curve", θ_A is defined by angle of curvature at the rightmost point of the gait pattern, and θ_B is defined by the angle of curvature at the equivalent point at same height on the vertical axis as θ_A. For the "Digitigrade locomotion" and "Step climbing", θ_A is defined by the angle of curvature at the rightmost point of the gait pattern, and θ_B is defined by the angle of curvature at the leftmost point. For the "Obstacle avoidance" and "Jam avoidance", θ_A and θ_B are defined by the angle of curvature at two points of the gait pattern that intersects an arbitrary threshold set on the vertical height axis whose value is chosen to be lower than the height of the rightmost point of the gait.

In the case of "Drilling motion", θ_B is defined by the angle of curvature at the lowest vertical height point of the gait pattern and θ_A is defined by the angle of curvature of an arbitrary point on the right-center of the gait pattern. Such atypical angular values are utilized for the "Drilling motion" because the pattern represents a tooling task that is very different from walking, as it is the case in the other gait cycles. The initial states of each PHASE are presented in Table 3 and the final states of each PHASE are the initial states of next PHASE. By utilizing these initial and final states and the trajectory generator designed in Section 3,

Table 2 The switching angles of support leg and idling leg.

Switch angle	Default curve	Digitigrade locomotion	Obstacle avoidance	Jam avoidance	Step climbing	Drilling motion
θ_A (rad)	1.05	1.09	0.91	0.88	1.24	3.00
θ_B (rad)	5.55	4.97	$0.04+2\pi$	5.70	$5.05-2\pi$	$4.89-2\pi$

Table 3 Initial states of each leg for the synchronization (n : count of loop of PHASE, $\eta=(\theta_A-\theta_B+2\pi)/3$).

State	PHASE 1 (rad)	PHASE 2 (rad)	PHASE 3 (rad)	PHASE 4 (rad)	Speed (rad/s)
Left fore	$\theta_A+2\pi n$	$\theta_B+2\pi n$	$\theta_B+\eta+2\pi n$	$\theta_A-\eta+2\pi(n+1)$	η/T
Left back	$\theta_A-2\pi(n-1)$	$\theta_A-\eta-2\pi(n-1)$	$\theta_B+\eta-2\pi n$	$\theta_B-2\pi n$	$-\eta/T$
Right fore	$\theta_B+\eta+2\pi(n-1)$	$\theta_A-\eta+2\pi n$	$\theta_A+2\pi n$	$\theta_B+2\pi n$	η/T
Right back	$\theta_B+\eta-2\pi n$	$\theta_B-2\pi n$	$\theta_A-2\pi n$	$\theta_A-\eta-2\pi n$	$-\eta/T$

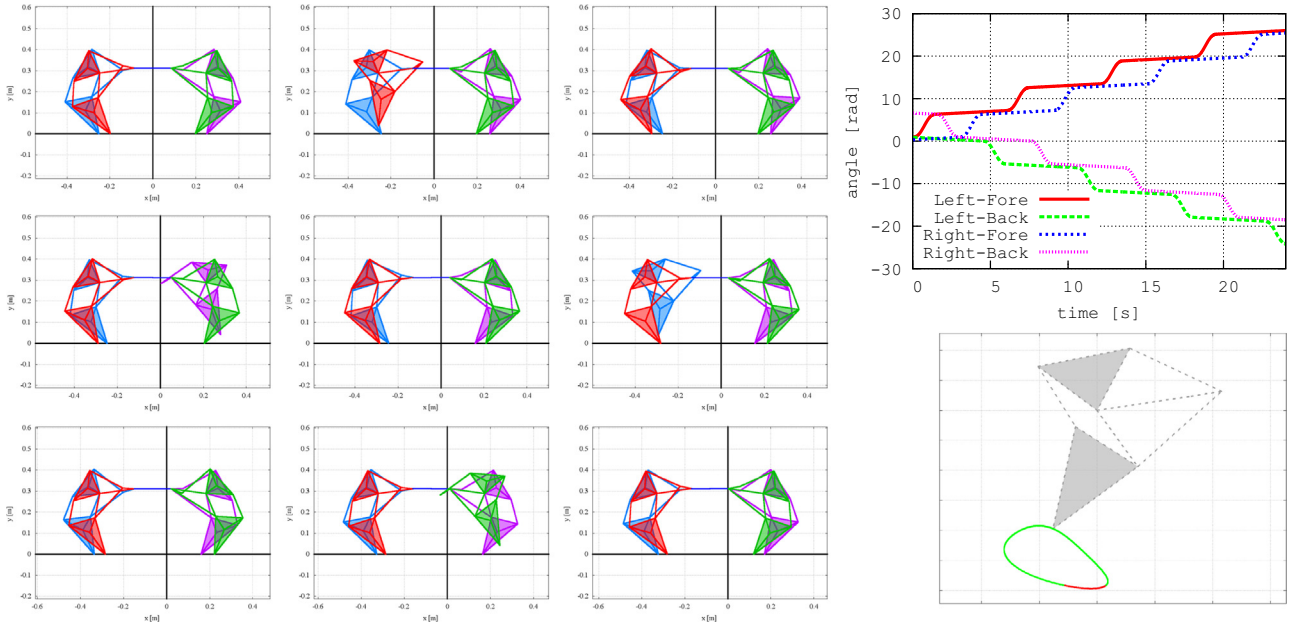

Fig. 4 The simulation result of the synchronization for the stable walking (*left*). *Red leg*: Left-Fore leg. *Green leg*: Left-Back. *Blue leg*: Right-Fore. *Purple leg*: Right-Back. The generated trajectories for the driving link (*right-top*). The gait pattern of "Obstacle avoidance" (*right-bottom*).

Table 4 Results of the static stability analysis of the synchronization.

Gait pattern	PHASE 1	PHASE 2	PHASE 3	PHASE 4
Default curve	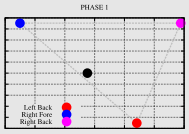	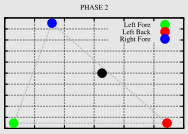	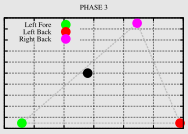	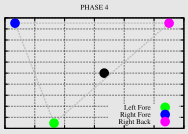
Digitigrade locomotion	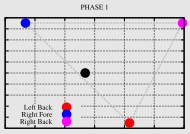	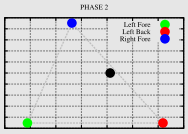	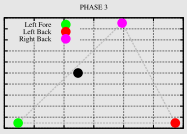	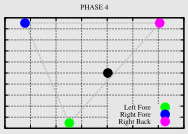
Obstacle avoidance	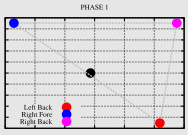	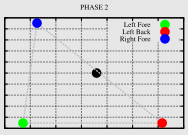	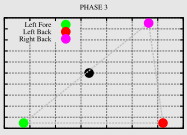	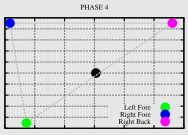
Jam avoidance	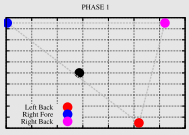	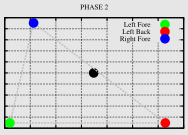	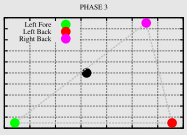	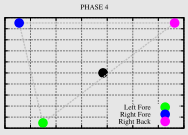
Step climbing	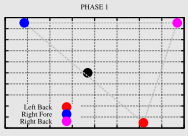	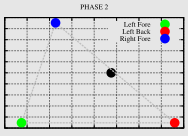	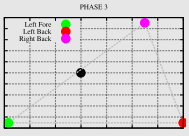	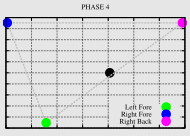
Drilling motion	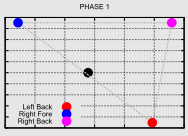	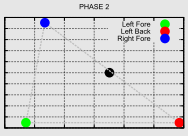	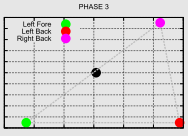	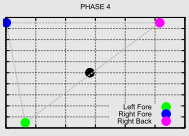

the stable walking for the obstacle avoidance gait can be realized as shown in Fig. 4.

The proposed trajectory generator is useful in realizing a set of stable walking gaits achieved through synchronization of leg movements.

5. Static stability analysis of the realized gaits

This section presents the results of the static stability analysis for the intermediary phases of the walking gaits considered in this study. Relation between the support legs and center of gravity (COG) of the robot is presented in Table 4 where black points represent the COG of the robot, and red points, blue points, green points and purple points represent the contact point of the support legs, and the gray line represents the static stability zone.

These static stability results show that the proposed approach generates walking gaits whose constituent phases possess static stability – observed by the existence of center of gravity within the static stability zone. However, low stability margins are observed in Table 4 when computed by known evaluation methods [24–26]. This results from the fact that the idling leg moves on a specific plane, and movements outside it cannot be physically achieved or controlled. And, the fact is one of the big characterization of using the Jansen linkage mechanism. An ordinary leg mechanism installing some actuators on 1 leg consists of simple mechanisms, and realizes walking by seeking complexities for walking to a control system. Hence, the main challenge has been to design an application capable of keeping high stability. On the other hand, our platform has utilized the Jansen linkage mechanism as the leg mechanism. The Jansen linkage mechanism is capable of driving with 1-DOF, and realizes walking by seeking complexities for walking to a mechanical system. Therefore, the main challenge is to design a simple application as much as possible with maintaining the minimum stability. That is, the stability and the complexity of the application are always trade-off. Thus, the issues about the stability of the platform should be discussed. But, several solutions can be identified in order to improve such margins while maintaining the simplicity of control, for example, adding a horizontal moving weight in the body that moves away from the idling leg. In any case, this is an aspect that deserves further research.

6. Characterization of gait transition

We have so far discussed leg synchronization problem associated with gait generation and stability analysis for a set of synthesized walking gaits in a reconfigurable Jansen platform. Another key challenge in such shape shifting robots is to realize a stable gait transition. Two approaches have been put forward in the literature. Ref. [27] proposes a strategy that involves gait transition at rest (Static gait

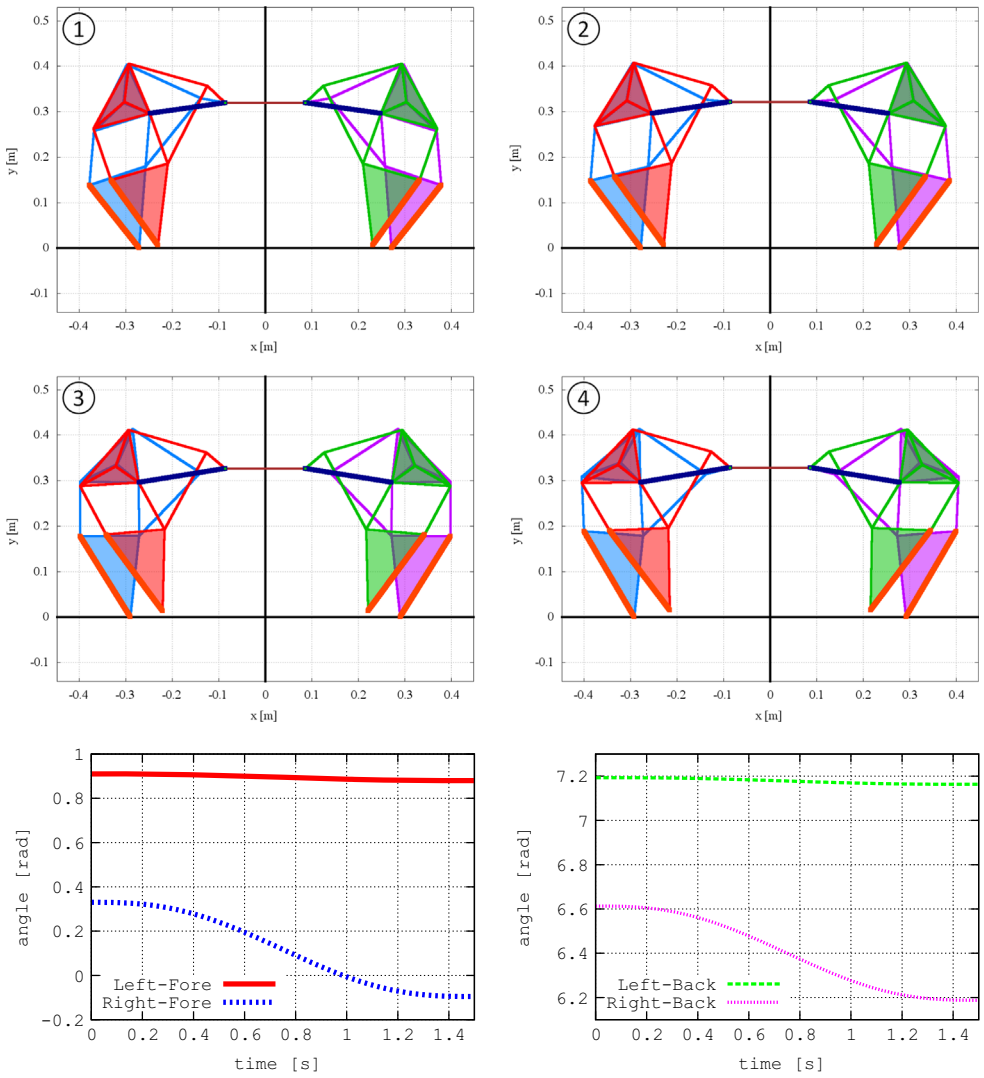

Fig. 5 The transformation from "Obstacle avoidance" to "Jam avoidance" by Static Transformation. *Top*: Some steps of the transformation. The binary links of variable dimension are highlighted in orange-red and dark-blue. *Bottom*: The generated trajectories for the driving link.

Table 5 The initial and final state of the idling leg in the transformation in walking ($f(\theta, l)$: Length of $\overline{P_1P_8}$ [6]).

Variables		Initial states	Final states
θ	**Position** (rad)	θ_A	$\theta_B^{'}$
	Speed (rad/s)	$\pm\eta/T$	$\pm\eta^{'}/T$
l	**Position** (%)	$\overline{P_iP_j}$: a	$\overline{P_iP_j}$: 0
		$\overline{P_mP_n}$: 0	$\overline{P_mP_n}$: b
	Speed (%/s)	***0***	***0***
y	**Position** (m)	0	$f(\theta_A, l) - f(\theta_B^{'}, l^{'})$
	Speed (m/s)	0	0

transition) and [28] studies gait transition while in motion (Dynamic gait transition). The static gait transition has obvious advantages allowing switching of gaits within a restricted space as well as increased stability due to the robot platform being at rest. On the other hand, the dynamic gait transition allows for a seamless switching of gaits as the process happens in motion without any disruption. In this paper, we present our experiments utilizing both the static and dynamic approaches to gait transition. Both the approaches are compatible with the proposed trajectory generator where the transition of gaits is achieved by substituting the initial and final states together with the link dimension and angle of the driving link into the trajectory generator as discussed in Section 4. These sets of associated variables are then defined namely, θ represents the angle of the driving link, l represents the length of the variable link (for example, it is $\overline{P_1P_2}$ and $\overline{P_7P_8}$ in the case of transitioning from "Obstacle avoidance" into "Jam avoidance", see details in [6]), and y represents the height of whole leg. In addition, a prime added $'$ to these variables represents the state after transition.

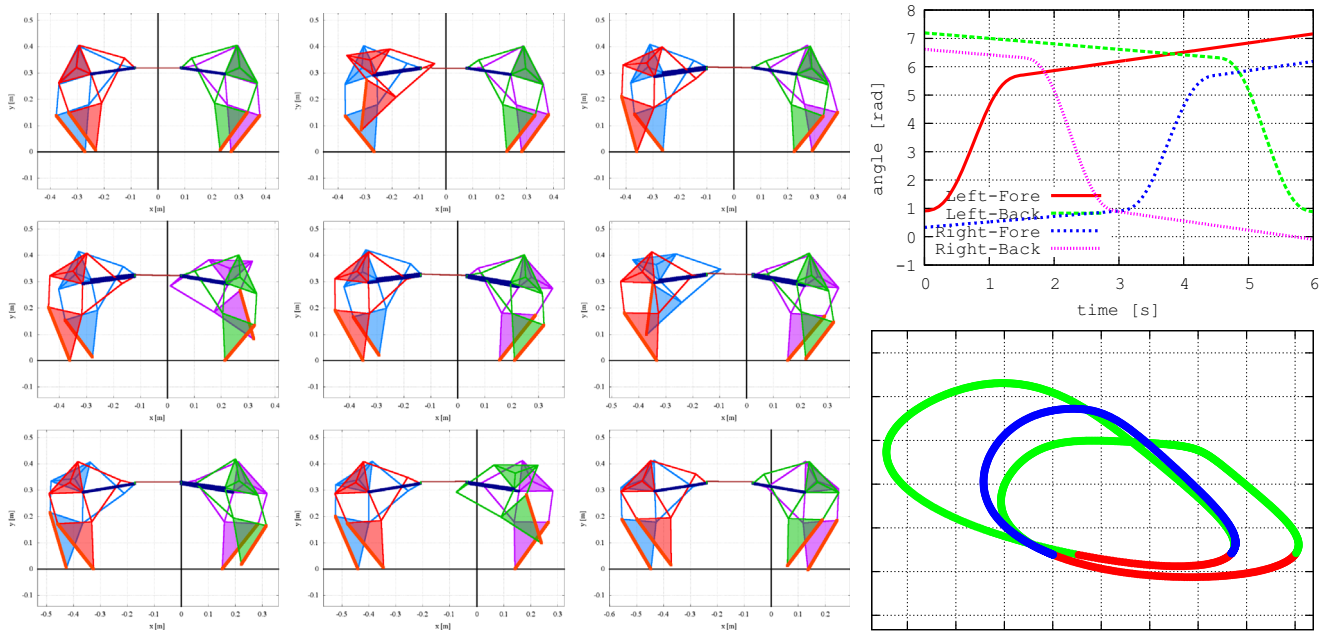

Fig. 6 The transformation from "Obstacle avoidance" to "Jam avoidance" by Transformation in Walking. *Left*: Some steps of the transformation. The binary links of variable dimension are highlighted in orange-red and dark-blue. *Right-Top*: The generated trajectories for the driving link. *Right-Bottom*: The foot trajectory of leg "Left-Fore". The green and red line represent the trajectory of the idling leg and the support leg, respectively. The blue line represents the foot trajectory under the transformation.

6.1. Gait transition I - *static gait transition*

In this method, the robot changes gait while at rest involving transitioning of all legs at the same time while in contact with the ground. Such an approach where the initial state of gait transition corresponds to the resting PHASE is set to ensure increased stability. In general, a gait transition in this case would start with bringing the robot platform to rest at the initial state of either one of the PHASE, realize gait transition and restart motion upon completion of the structural changes needed for the gait transition.

In the case of transitioning from PHASE i $(i = 1, \ldots, 4)$ of pattern A to another pattern B; θ, $\boldsymbol{l}$ on the PHASE i $(i = 1, \ldots, 4)$ are defined as the angle of the driving link and length of the variable link at the initial state and θ', $\boldsymbol{l}'$ are defined as the values at the final state. These values are then fed to the proposed trajectory generators to achieve synchronization of legs for stable gait transition. Since it is assumed that the robot is at rest at the initial and final states, their velocity components are defined as $\dot{\theta} = 0$, $\dot{\theta}' = 0$, $\dot{\boldsymbol{l}} = 0$, $\dot{\boldsymbol{l}}' = 0$. Fig. 5 presents the gait transition from "Obstacle avoidance" into "Jam avoidance" at rest as an example. The binary links of variable dimension are highlighted in orange-red and dark-blue in Fig. 5.

6.2. Gait transition II - *dynamic gait transition*

In this method, the gait transition occurs while in motion and specifically during walking in this case. The proposed trajectory generator as discussed in the previous sections is utilized to achieve synchronization of the legs needs for stable gait transition. Gait transition in this case may involve legs in different configurations leading to large height difference between the supporting legs irrespective of having the same height of θ_A and θ_B set during the synchronization phase. Other negative implications could involve supporting legs not coming in contact with the ground or idling leg coming in contact with the ground. To avoid these pitfalls, the height of the leg after transition is set to the same height of θ_A that exists before gait transition. In our previous study [6], the height of each leg in specific configuration was dependent directly on the angle of the driving link and the link dimensions while the gait transition always occurred at the lowest point of that gait pattern. On the other hand, in this study, the height of each leg in specific configuration is also adapted utilizing the designed trajectory generator as the gait transition occurs in the idling phase while the leg is not in contact with the ground.

The initial and final states of the idling leg are shown in Table 5, where $f(\theta, \boldsymbol{l})$ represents $\overline{P_1P_8}$ for the angle of the driving link θ and the link dimensions $\boldsymbol{l}$. And, the ones for the supporting legs are shown in Table 3, where the parameters of a transformed gait are used for the legs upon transition. Fig. 6 presents the dynamic gait transition from "Obstacle avoidance" to "Jam avoidance" as an example. The binary links of variable dimension and the vertical movement of the grounded revolute joint centers are highlighted in orange-red, dark-blue, and light-green in Fig. 6.

7. Stability analysis of gait transition

This section presents the static stability analysis for all gait transitions synthesized with our reconfigurable Jansen platform. Firstly, we will discuss the stability analysis of the static gait transitions where the transformation occurs always on the initial state of the PHASE. As shown in Fig. 3 and Table 3, the

Table 6 Results of the static stability analysis of the gait transition II - *dynamic gait transition*.

Default curve				
Digitigrade locomotion	**Obstacle avoidance**	**Jam avoidance**	**Step climbing**	**Drilling motion**
Digitigrade locomotion				
Default curve	**Obstacle avoidance**	**Jam avoidance**	**Step climbing**	**Drilling motion**
Obstacle avoidance				
Default curve	**Digitigrade locomotion**	**Jam avoidance**	**Step climbing**	**Drilling motion**
Jam avoidance				
Default curve	**Digitigrade locomotion**	**Obstacle avoidance**	**Step climbing**	**Drilling motion**
Step climbing				
Default curve	**Digitigrade locomotion**	**Obstacle avoidance**	**Jam avoidance**	**Drilling motion**
Drilling motion				
Default curve	**Digitigrade locomotion**	**Obstacle avoidance**	**Jam avoidance**	**Step climbing**

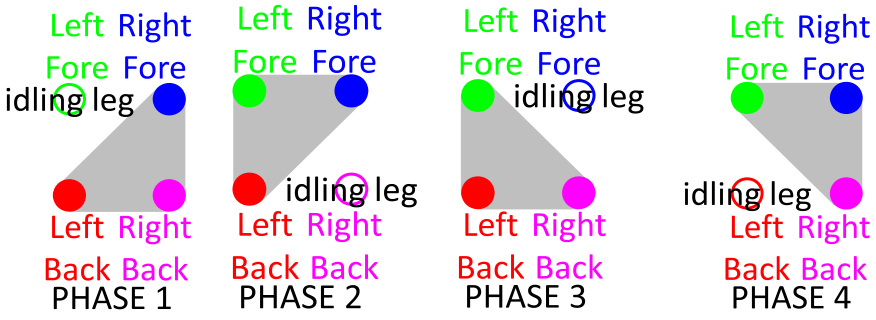

Fig. 7 The variety of the supporting leg polygon of the quadruped robot. The gray area represents the static stability zone.

robot would maintain stability in the case of static gait transitions given that the legs are always in contact with the ground. Also, the use of sliding screw mechanism for achieving structural reconfiguration of the platform prohibits any instantaneous gait transitions and associated stability issues. As for the stability during dynamic gait transition, the relationship between the support legs and COG of the robot for all gait transitions are presented in Table 6. In case of PHASE 1 and PHASE 4, the static stability would be maintained as illustrated in Table 4 given that all support legs are in the same configuration before and after gait transition. Hence, the focus of our further discussion will be on the static stability analysis in the PHASE 2 and PHASE 3. Table 6 presents the stability analysis with respect to PHASE 2 where the black points represent the COG of the robot, whereas red points, blue points, green points and purple points represent the contacting points of the support legs, and gray line represents the static stability zone. From Table 6, it can be inferred that the proposed approach ensures stable gait transition in PHASE 2 while walking as the center of gravity always remains within the static stability zone.

Our quadruped robot always walks with three support legs and one idling leg forming a triangular supporting leg polygon. For such a configuration, the stability of the robot would be ensured if the COG falls within the supporting leg polygon. Our case involves four potential variants of triangular polygons as presented in Fig. 7. When the COG of the robot exists at its center, then the positional relationship between a line connecting the two legs in opposing corners to which the COG is nearest and the COG directly impacts the static stability. In general as shown in Fig. 8, if the COG exists inside the triangular polygon formed by the supporting legs and the line connecting the two legs in opposing corners to which the COG is nearest, then the robot is statically stable (Fig. 8(a)) else unstable (Fig. 8(b)). For situations involving gait transitions as shown in Fig. 9 from gait *A* to gait *B*, our approach ensures that two of the supporting legs in opposing corners would always have the same configuration. Such an approach ensures static stability while gait transition in motion with respect to PHASE 3. Thus, the static stability of the dynamic gait transition can be achieved by realizing static stability of the realized gaits and the stability in PHASE 1–4 of the gait transition.

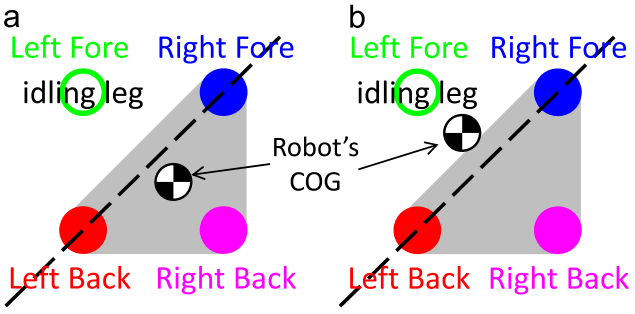

Fig. 8 The positional relationship between a line on the 2 legs in opposing corner and the COG which is relevant to the static stability. If the COG exists in side of the support leg than the line, the robot is static stable.

8. Conclusion

An original design approach has been presented in this paper towards the development of a trajectory generator that realizes a set of stable walking gaits and gait transition for a reconfigurable Jansen platform. We have discussed a novel strategy to address the leg synchronization problem in this reconfigurable design and gait transition. Stability analysis is presented for prospective six gait patterns generated and all gait transitions by the reconfigurable platform and results discussed in view of validating the proposed approach. The proposed method has achieved the synchronization of the gait patterns as well as the gait transition between the gait patterns by the simple application consisting of only one trajectory generator. And, the designed application is applicable for the synchronization and the gait transitions, even though new gait patterns are explored in the future works. While it has been shown that the minimum static stability of both the synchronization and the gait transitions, new challenges for higher stability have been raised. The ability to adapt to situations and produce appropriate stable gaits and switch between gaits would extend the capabilities of the robot beyond their intended application. A four-legged robot is currently being constructed to validate the robustness of the produced gaits and control approaches for real world deployments.

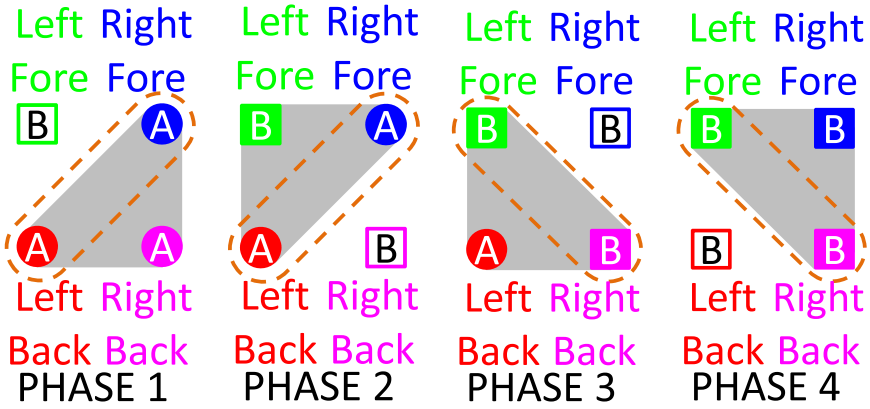

Fig. 9 The variety of combination of the gait pattern. "A" within circle and "B" within square represents a gait pattern A and a gait pattern B, respectively.

Acknowledgment

This work was supported by the SUTD-MIT International Design Center under Grants IDG31200110 and IDD41200105, and by the SUTD-ZJU Research Center.

References

[1] A. Kamimura, H. Kurokawa, E. Yoshida, S. Murata, K. Tomita, S. Kokaji, Automatic locomotion design and experiments for a modular robotic system, IEEE/ASME Trans. Mechatron. 10 (3) (2005) 314–325.
[2] C. Paul, J.W. Roberts, H. Lipson, F.V. Cuevas, Gait production in a tensegrity based robot, in: 12th IEEE International Conference on Advanced Robotics, 2005, pp. 216–222.
[3] K. Tsujita, T. Kobayashi, T. Inoura, T. Matsuda, Gait transition by tuning muscle tones using pneumatic actuators in quadruped locomotion, in: The 2008 IEEE/RSJ International Conference on Intelligent Robots and Systems (IROS), 2008, pp. 2453–2458.
[4] C. Paul, Morphological computation: a basis for the analysis of morphology and control requirements, Robot. Auton. Syst. 54 (8) (2006) 619–630.
[5] J.G. Cham, J.K. Karpick, M.R. Cutkosky, Stride period adaptation of a biomimetic running hexapod, Int. J. Robot. Res. 23 (2) (2004) 141–153.
[6] S. Nansai, N. Rojas, R.E. Mohan, R. Sosa, Exploration of adaptive gait patterns with a reconfigurable linkage mechanism, in: The 2013 IEEE/RSJ International Conference on Intelligent Robots and Systems (IROS), 2013, pp. 4661–4668.
[7] G.C. Haynes, A.A. Rizzi, Gaits and gait transitions for legged robots, in: Proceedings 2006 IEEE International Conference on Robotics and Automation, 2006 (ICRA2006), 2006, pp. 1117–1122.
[8] C.P. Santos, V. Matos, Gait transition and modulation in a quadruped robot: a brainstem-like modulation approach, Robot. Auton. Syst. 59 (9) (2011) 620–634.
[9] H. Kimura, S. Akiyama, K. Sakurama, Realization of dynamic walking and running of the quadruped using neural oscillator, Auton. Robots 7 (3) (1999) 247–258.
[10] V. Kee, N. Rojas, M.R. Elara, R. Sosa, Hinged-tetro: A self reconfigurable module for nested reconfiguration, in: 2014 IEEE/ASME International Conference on Advanced Intelligent Mechatronics (AIM), 2014, pp. 1539–1546.
[11] C. Heng, R. de Leon, Treadmill training enhances the recovery of normal stepping patterns in spinal cord contused rats, Exp. Neurol. 216 (1) (2009) 139–147.
[12] F. Lacquaniti, R. Grasso, M. Zago, Motor patterns in walking, Physiology 14 (4) (1999) 168–174.
[13] J. Johnson, J. Burton, Animal Tracks and Signs: Track Over 400 Animals From Big Cats to Backyard Birds, National Geographic Children's Books, Des Moines, IA, 2008.
[14] K. Komoda, H. Wagatsuma, A study of availability and extensibility of theo jansen mechanism toward climbing over bumps, in: The 21st Annual Conference of the Japanese Neural Network Society, 2011, pp. 3–28.
[15] K. Erbatur, A. Okazaki, K. Obiya, T. Takahashi, A. Kawamura, A study on the zero moment point measurement for biped walking robots, in: The 7th International Workshop on Advanced Motion Control, 2002, pp. 431–436.
[16] S. Kajita, F. Kanehiro, K. Kaneko, K. Fujiwara, K. Harada, K. Yokoi, H. Hirukawa, Biped walking pattern generation by using preview control of zero-moment point, in: The 2003 IEEE International Conference on Robotics and Automation, 2003, pp. 1620–1626.
[17] P. Sardain, G. Bessonnet, Forces acting on a biped robot center of pressure—zero moment point, IEEE Trans. Syst. Man Cybern. 34 (5) (2004) 630–637.
[18] S. Nansai, R.E. Mohan, M. Iwase, Dynamic analysis and modeling of Jansen mechanism, Procedia Eng. 64 (2013) 1562–1571.
[19] A.J. Ingram, A new type of mechanical walking machine, Rand Afrikaans University.
[20] Y. Okazaki, M. Yamamoto, M. Komatsu, Y. Tsusaka, Y. Adachi, Development of a human safe, multi-degree-of-freedom robot arm technology using pneumatic muscles, J. Robot. Soc. Jpn. 28 (3) (2010) 62–70 (in Japanese).
[21] Y. Noguchi, M. Iwase, S. Hatakeyama, M. Izutsu, A yoyo trick realized by parallel-link manipulator, in: The 39th Annual Conference of the IEEE Industrial Electronics Society, 2013, pp. 4049–4054.
[22] Y. Takeda, M. Okada, Development of a jumping robot with a non-circular gear, in: The 2012 JSME Conference on Robotics and Mechatronics, vol. 3 (12), 2012, pp. 2A2–V04.
[23] H. Nagashiro, Y. Nomura, Y. Kinouchi, A neural network model for quadruped gait generation and transitions, Neurocomputing (38–40) (2001) 1469–1475.
[24] K. Yoneda, S. Hirose, Tumble stability criterion of a walking machine, J. Robot. Soc. Jpn. 14 (4) (1996) 517–522 (in Japanese).
[25] S. Hirise, H. Tsukakoshi, K. Yoneda, Static stability criterion for walking robots on irregular terrains, J. Robot. Soc. Jpn. 16 (8) (1998) 1076–1082 (in Japanese).
[26] D.A. Messuri, C.A. Klein, Automatic body regulation for maintaining stability of a legged vehicle during rough-terrain locomotion, IEEE J. Robot. Autom. RA-1 (3) (1985) 132–141.
[27] S.Y. Shen, C.H. Lin, C.C. Cheng, J.C. Lu, S.F. Wang, P.C. Lin, Design of a leg-wheel hybrid mobile platform, in: The 2009 IEEE/RSJ International Conference on Intelligent Robots and Systems (IROS), 2009, pp. 4682–4687.
[28] G. Endo, S. Hirose, Study on roller-walker (system integration and basic experiments), in: The 1999 IEEE International Conference on Robotics & Automation (ICRA), 1999, pp. 2032–2037.